Photoluminescence and local structure of Ge nanoclusters on Si without a wetting layer

A. P. Li
Condensed Matter Sciences Division, Oak Ridge National Laboratory, Oak Ridge, Tennessee 37831, USA

F. Flack and M. G. Lagally
Department of Physics, The University of Wisconsin-Madison, Madison, Wisconsin 53706, USA

M. F. Chisholm and K. Yoo
Condensed Matter Sciences Division, Oak Ridge National Laboratory, Oak Ridge, Tennessee 37831, USA

Zhenyu Zhang and H. H. Weitering
Condensed Matter Sciences Division, Oak Ridge National Laboratory, Oak Ridge, Tennessee 37831, USA and Department of Physics and Astronomy, University of Tennessee, Knoxville, Tennessee 37996, USA

J. F. Wendelken
Condensed Matter Sciences Division, Oak Ridge National Laboratory, Oak Ridge, Tennessee 37831, USA
(Received 6 October 2003; revised manuscript received 5 January 2004; published 18 June 2004)

Photoluminescence (PL) originating from single layers of Ge nanoclusters grown on Si(100) via a buffer layer-assisted growth method is investigated. The nanoclusters are characterized by the absence of a wetting layer. They are quasi-zero-dimensional with tunable sizes and exhibit a high cluster density compared to Ge nanoclusters that are formed from the standard Stranski-Krastanov growth. Samples with different cluster sizes show strong and sharp PL in the near infrared. The excitation power and temperature dependencies of PL spectra indicate that the optical transitions are bound-to-bound in nature, suggesting that defects rather than the band structures are associated with the luminescence centers. High-resolution transmission electron microscopy (TEM) reveals that these nanoclusters are amorphous, which could explain the strong defect-related emission.

DOI: 10.1103/PhysRevB.69.245310 PACS number(s): 61.46.+w, 68.37.Lp, 78.67.Hc, 78.55.Ap

Self-assembled formation of Ge nanoclusters on Si has been intensively studied as it could promote the development of Si-based optoelectronics. Although remarkable successes have been achieved,[1–3] it remains challenging to create zero-dimensional (0D) Ge clusters on Si(100) with small, dense, and uniform dot formation. One of the dominant growth mechanisms is the Stranski-Krastanov (SK) growth mode, which leads to the formation of coherently-strained, pseudomorphic three-dimensional islands on top of a two-dimensional wetting layer. Germanium SK dots grown on Si typically have lateral dimensions of 10–50 nm and are 1–5 nm in height. Their larger lateral size means that quantum confinement effects are mostly determined by the dot sizes along the growth direction. Moreover, SK growth implies the formation of a 2D Ge wetting layer beneath the dots.[4–6] Wetting layer formation results from the lattice mismatch (4.2%) between Si and Ge, which allows strained layer-by-layer growth up to a certain critical thickness, followed by a strain-relieve transition and 3D island formation. The wetting layer is electronically coupled to the Ge islands which reduces quantum confinement and electronically couples neighboring quantum dots. This likely reduces their potential for optoelectronic performance.

We have recently applied a buffer layer-assisted growth method to fabricate Ge nanoclusters.[7] The nanoclusters produced by this method are characterized by the absence of a wetting layer. They are quasi-zero-dimensional, have tunable sizes, and the cluster density is high compared to that of Ge nanoclusters formed via conventional SK growth. In this paper, we report the photoluminescence (PL) from the Ge nanoclusters grown by this buffer layer-assisted approach. The PL spectra are remarkably different from those of SK dots. The origins of the PL are correlated with the structural properties of the nanoclusters.

The Ge nanoclusters were grown on a Si(100) substrate in an ultrahigh vacuum (UHV) system with base pressure of 2×10^{-10} Torr. To inhibit direct interactions of deposited atoms with the substrate during Ge nanocluster growth, we have used a layer of condensed Xe as a buffer between the clusters and the substrate. The buffer layer-assisted growth method has been described in detail previously.[7–10] After cooling a clean Si(100) substrate to 10 K in UHV, buffer layers of condensed Xe ranging from 4 to 40 monolayers (ML) were formed by a ~20 to 200 Langmuir exposure to pure Xe gas (99.995%). Next, a flux of pure Ge atoms was deposited on top of the Xe buffer layer. Due to the low surface free energy of Xe, these atoms exhibit extremely high surface mobility, compared to the surface mobility on a Si substrate, and easily nucleate into small, 3D nanoclusters. Finally, the sample was warmed to room temperature to remove the buffer layer and to softly land the nanoclusters onto the Si substrate.

All samples were examined *in situ* by scanning tunneling microscopy (STM) at room temperature to ensure that the substrate is atomically smooth before nanocluster fabrication and to examine the morphology of the Ge nanoclusters after

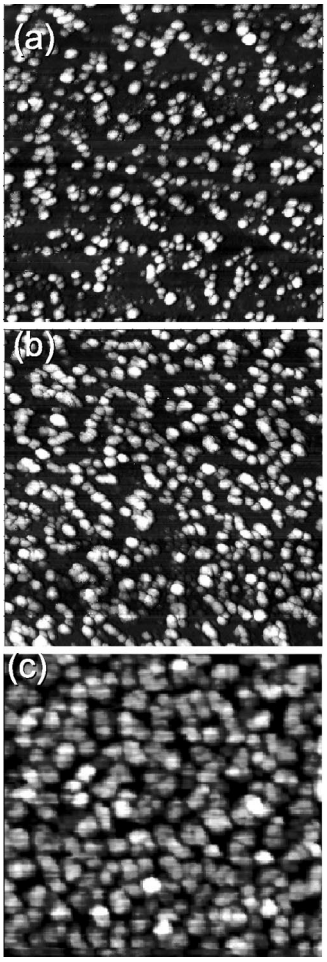

FIG. 1. 100 nm × 100 nm STM images of Ge nanoclusters fabricated with the buffer layer-assisted growth method with nominal Ge thickness of (a) 0.3 ML, (b) 0.6 ML, and (c) 6 ML. The Xe buffer layer thickness was the same in all cases.

deposition. After formation of the Ge nanoclusters, an amorphous Si capping layer was deposited at room temperature. The samples were then removed from the UHV chamber for PL measurements. Samples were cooled to 15 K in a closed-loop helium cryostat and irradiated with the 514.5 nm line of an Ar^+-laser with power densities ranging from 1 to 5 W/cm^2. The luminescence from the sample was dispersed with a 1m grating monochromator (Spex) with sub-angstrom resolution. The PL spectra were measured with a liquid-nitrogen-cooled Ge detector (North Coast) using standard phase lock detection techniques.

The samples were also examined using the high resolution *Z*-contrast imaging technique in a scanning transmission electron microscope (TEM, VG Microscopes HB501U) operated at 100 kV. This microscope, equipped with a NION aberration corrector, is capable of forming an electron probe of 1-Å diameter. The *Z*-contrast technique provides atomic resolution images by effectively illuminating successive atomic columns as the electron probe is scanned across the thinned sample. This leads to directly interpretable images with strong compositional sensitivity.

Figure 1 displays STM images of Ge nanoclusters with nominal coverages of 0.3, 0.6, and 6 ML. The thickness of

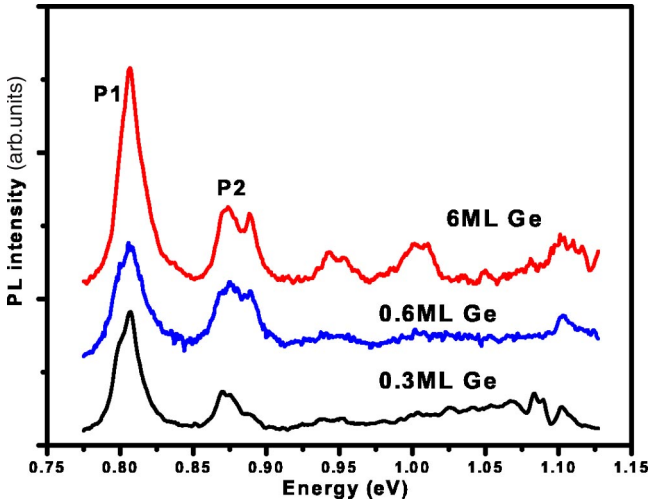

FIG. 2. PL spectra of Ge nanoclusters with nominal Ge thickness of (a) 0.3 ML, (b) 0.6 ML, and (c) 6 ML. The spectra were measured at 15 K.

the Xe buffer layer that was used in the fabrication process is 6 ML in each case. These Ge nanoclusters exhibit an average lateral size of 2.0 nm and a height of 0.4 nm at a nominal Ge coverage of 0.3 ML. At a Ge coverage of 6 ML, the clusters are 7.5 nm in diameter and 1.2 nm in height. In all cases, even when Ge coverage is much less than the critical thickness (the onset of SK dot growth occurs at 3–5 ML Ge depending on growth conditions), the nanoclusters are isolated. STM images reveal the pristine Si surface in areas between nanoclusters. The nominal Ge coverage derived from the nanocluster is consistent with this model. As seen in previous buffer layer-assisted growth experiments, the mediation of the Xe buffer prevents direct interactions of deposited atoms with the substrate and no strained wetting layer is formed in between the nanoclusters.[7–10]

The PL spectra from these samples are shown in Fig. 2. The dominant bands are centered at 0.806 eV (*P*1) and 0.873 eV (*P*2) with a full width at half maximum (FWHM) of 20 meV, which is very sharp in comparison to the PL spectra from SK dots (FWHM of 60–100 meV).[2–5] However, the energies of *P*1 and *P*2 are independent of cluster size. Since the clusters are much smaller than SK dots and should therefore exhibit much stronger quantum confinement, the absence of size effects on the PL peak energy suggests that the PL is probably not directly associated with the band structure of the clusters. The emission band at around 1.1 eV is attributed to the phonon-assisted recombination of the free-exciton in the Si substrate.[2,4,11,12] The PL bands at around 0.94 and 1.00 eV, which appear on the 6 ML Ge sample and also on other high Ge-coverage samples, correspond to the excitonic no-phonon and transverse-optical-phonon-assisted transitions of 2D Ge in Si.[13,14] This implies the possibility that 2D Ge starts to form as the Ge coverage increases. However, TEM analysis (discussed later) shows no evidence of a pseudomorphic Ge layer. Hence, these PL features cannot be attributed to a conventional Ge wetting layer.

The excitation-power dependence of the PL from a sample with 0.5 ML Ge deposited with 6 ML Xe as a buffer

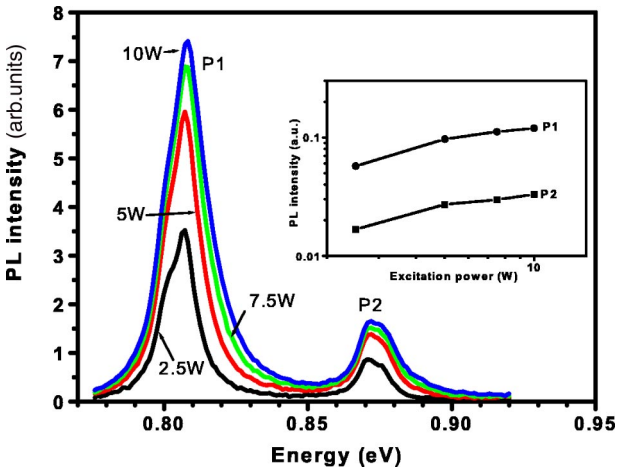

FIG. 3. Excitation power dependence of PL spectra from Ge nanocluster formation on Si(100) with a buffer layer-assisted growth method. The nominal Ge thickness is 0.5 ML, and the Xe buffer thickness is 6 ML. The inset shows the excitation dependence of the integrated PL intensity for the same sample.

layer is shown in Fig. 3. In contrast to the PL behavior from SK dots, the peak energies of both $P1$ and $P2$ do not shift with increasing excitation power from 1 to 5 W/cm^2. Coherent strain in SK-grown dots normally produces a type-II band alignment, in which electrons and holes occupy spatially separated regions.[2–5,10,11] Band bending at the interfaces of type-II structures would blueshift the PL signal as greater excitation power density increases the carrier density.[15–17] Such a blueshift is not observed in nanoclusters prepared with the buffer layer-assisted growth method, and it is thus likely that *these clusters do not possess a type-II band alignment at the Ge/Si interface*. This would also be consistent with the fact that negligible strain exists at the Ge nanocluster/Si interface as a result of the Xe buffer layer-assisted growth process. The excitation curves, shown in the inset of Fig. 3, reveal sublinear ($\sim$0.50) power exponents for the $P1$ and $P2$ bands. Sublinear power exponents with a power exponent of $\sim$0.78 have previously been attributed to type-II band alignment with a limited density of localized states for excitons.[4,15] Increased localization of the radiative centers would lead to a smaller power exponent. A power exponent of $\sim$0.66, which is closer to our value, has been observed from SiGe dots at high excitation power density and has been attributed to direct competition between the Auger and radiative recombination channels in the dots.[2,12,18] Considering the fact that the peak energy does not blueshift at high excitation power, it is plausible to also attribute the observed sublinear power exponent to a competition between localized radiative recombination processes and Auger recombination channels.

Figure 4(a) shows the integrated PL intensity of band $P1$ and $P2$ as a function of measurement temperature. The PL intensity starts to decrease rapidly at 75 K for both bands. The thermal activation energy E_A can be obtained from the Arrhenius plot of the PL intensity. The deduced E_A is 18.6 meV for $P1$ and 11.2 meV for $P2$. The obtained E_A would correspond to the energy barrier for excitons escaping from radiative centers to nonradiative recombination centers.

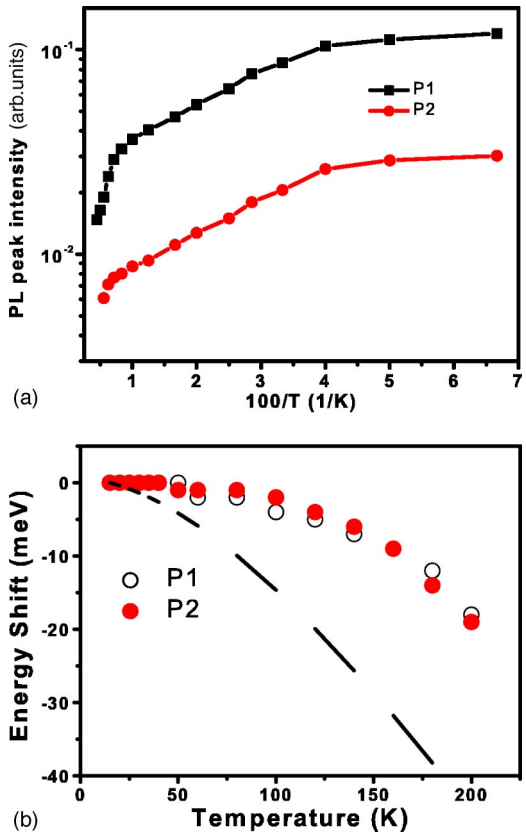

FIG. 4. The temperature dependence of PL spectra from Ge nanoclusters with 0.5 ML Ge and Xe buffer layer thickness is 6 ML. (a) Arrhenius plot of PL integrated intensity for bands $P1$ and $P2$ as a function of measurement temperature. (b) The PL peak shift with temperature of the $P1$ and $P2$ bands. The dashed line represents the Varshni relationship of the Ge band gap.

The low activation energy would also imply weak confinement of excitons. The temperature dependence of the PL peak energy is shown in Fig. 4(b). The peak energies of the $P1$ and $P2$ bands redshift with temperature. However, the variations depart significantly from the Varshni relationships of the Ge band gap and the Si band gap.[19] This result again confirms that the $P1$ and $P2$ transitions are not associated with the Ge band edges or Si band edges, indicating *a "bound to bound" nature of the P1 and P2 transitions*. These localized luminescence centers likely originate from defect centers at the Ge/Si interface or defect centers inside the Ge clusters.

The PL behaviors show that the Ge nanoclusters fabricated with the buffer layer-assisted growth method do not have the usual type-II band alignment and that radiative recombination is not associated with band edges. To elucidate these unusual luminescence properties, we investigated the local structures at the Ge nanocluster/Si interface using TEM. Figure 5(a) displays a cross-sectional Z-contrast TEM image of the sample with 6 ML Ge, showing the structure of Ge nanoclusters sandwiched between the amorphous Si cap layer and crystalline Si substrate. A higher magnification image in Fig. 5(b) indicates that the Ge island makes an obtuse contact angle with the Si substrate. No coherent Ge layer between the Ge nanoclusters is observed, confirming the ab-

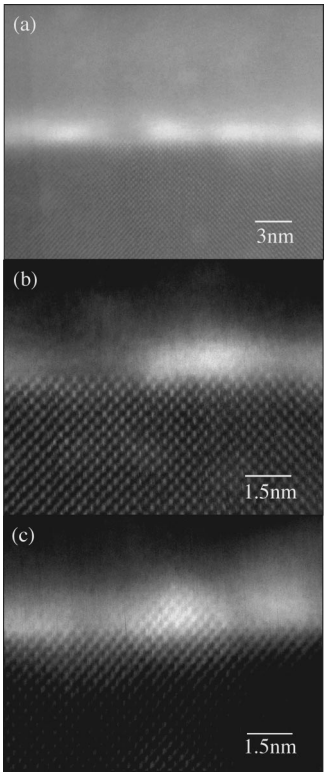

FIG. 5. Cross sectional *Z*-contrast images of 6 ML Ge deposited on 6 ML Xe buffer layer on Si(001). (a) Ge nanoclusters sandwiched between the Si substrate and an amorphous Si capping layer. (b) Higher magnification image showing an amorphous Ge cluster making an obtuse contact angle with the Si substrate. (c) Image of a Ge island after increased exposure to the electron beam of the microscope showing that the dot has crystallized and adopted a pseudomorphic structure relative to the Si substrate.

sence of a wetting layer. Moreover, no lattice coherence appears at the Ge nanocluster/Si interface and the Ge clusters are amorphous. The observed shape of the amorphous islands is different from the hut clusters with {510} facets normally seen when Ge is deposited on the Si(100) surface.[20] After increased exposure to the electron beam of the microscope, the amorphous Ge clusters crystallize. In Fig. 5(c), these Ge islands have become crystalline and adopted a pseudomorphic structure with respect to the Si substrate. Evidently, high-energy electron beam bombardment can induce an amorphous to crystalline phase transition in Ge nanoclusters. Furthermore, the recrystallized clusters tend to align to the Si substrate lattice.

To clarify the role of these amorphous Ge nanoclusters in the PL process, a reference sample was fabricated without the mediation of a Xe buffer layer. In this way, clustering was avoided and a uniform amorphous Ge layer of 6 ML equivalent coverage was deposited directly onto Si at 10 K, and subsequently capped with an amorphous Si layer at room temperature. The amorphous nature of the deposited Ge layer was confirmed with STM and low energy-electron diffraction (LEED). Under the same measurement conditions, only a weak PL emission band from the Si substrate (1.1 eV) appeared; the *P*1 and *P*2 bands were neither observed from the uniform Ge amorphous layer nor from the amorphous Si cap layer of the reference sample. The exclusive presence of *P*1 and *P*2 emission bands in the samples containing amorphous Ge nanoclusters indicates that these *amorphous clusters must play a critical role in the PL process*. A possible explanation of the PL is that excitons are generated in the Ge nanoclusters or in bulk Si, and then decay at defect centers that are located either within the dots or at the dot/Si interface. The presence of Ge nanoclusters produces high energy excitons, higher than the bulk Ge band gap energy, and a high density of interface states. This model has been used extensively to explain the luminescence properties from Si and Ge nanocluster systems.[21–25]

We have noticed that our observed *P*1 and *P*2 bands are in similar energy positions to the dislocation centers *D*1 and *D*2 in SiGe at 0.808 and 0.875 eV, respectively.[12,26,27] However, a direct link between *P*-bands and *D*-lines cannot be established from this work. Fukatsu *et al.*[12] reported that *D*-lines are associated with the Si band edges because their temperature dependence follows a Varshni dependence. However, as shown in Fig. 4(b), the temperature dependence of the *P*-bands deviates significantly from the Varshni relationship. Instead, the *P*-bands appear to originate from a bound-to-bound transition. Furthermore, *D*-lines only appear in strained crystalline materials, yet the *P*-bands in this work are associated with the presence of amorphous Ge clusters that should not introduce strain in the film. Finally, *D*-lines are related to dislocations whereas no dislocations are visible in TEM of our samples. Hence, the *P*-band luminescence is most likely associated with dangling-bond-type defect centers either within the amorphous quantum dots or at the *a*-Ge/Si interface.

In summary, we have reported the PL behavior of Ge nanoclusters on Si(100), fabricated using a buffer layer-assisted growth method. The diameters of the nanoclusters can be tuned from 2 to 8 nm by changing the Ge coverage. There is no wetting layer at the Ge nanocluster/Si interface. Samples with different cluster sizes show strong, sharp PL bands in the near infrared spectral region. The PL energy is independent of cluster size. The excitation power and temperature dependences of the PL spectra suggest a bound-to-bound nature for the PL transition, which is clearly different from the PL of SK dots that have a type-II band alignment. Although the PL is probably associated with defect centers, the Ge nanoclusters must play a role in the PL process. High-resolution electron microscopy indicates that these Ge nanoclusters are amorphous, but may be crystallized during electron beam irradiation.

This work was supported by ORNL under the LDRD Program, managed by UT-Battelle, LLC for the U. S. Department of Energy under Contract No. DE-AC05-00OR22725, and in part by the Petroleum Research Fund, administrated by the ACS (Grant No. ACS-PRF#32916-AC5).

[1] M. Kaestner and B. Voigtlaender, Phys. Rev. Lett. **82**, 2745 (1999).
[2] M. W. Dashiell, U. Denker, and O. G. Schmidt, Appl. Phys. Lett. **79**, 2261 (2001).
[3] O. G. Schmidt, C. Lange, and K. Eberl, Appl. Phys. Lett. **75**, 1905 (1999).
[4] J. Wan, G. L. Jin, Z. M. Jiang, Y. H. Luo, J. L. Liu, and L. Wang, Appl. Phys. Lett. **78**, 1763 (2001).
[5] H. Sunamura, N. Usami, Y. Shiraki, and S. Fukatsu, Appl. Phys. Lett. **66**, 3024 (1995).
[6] K. Brunner, Rep. Prog. Phys. **65**, 27 (2002).
[7] K. Yoo, A. P. Li, Z. Zhang, H. H. Weitering, F. Flack, M. G. Lagally, and J. F. Wendelken, Surf. Sci. **546**, L803 (2003).
[8] J. H. Weaver and G. D. Waddill, Science **251**, 1444 (1991).
[9] J. Shen, J. P. Pierce, E. W. Plummer, and J. Kirschner, J. Phys.: Condens. Matter **15**, R1 (2003).
[10] C. Haley and J. H. Weaver, Surf. Sci. **518**, 243 (2002).
[11] M. W. Dashiell, U. Denker, C. Mueller, G. Costantini, C. Manzano, K. Kern, and O. G. Schmidt, Appl. Phys. Lett. **80**, 1279 (2002).
[12] S. Fukatsu, Y. Mera, M. Inoue, K. Maeda, H. Akiyama, and H. Sakaki, Appl. Phys. Lett. **68**, 1889 (1996).
[13] V. Le Thanh, V. Yam, P. Boucaud, F. Fortuna, C. Ulysse, D. Bouchier, L. Vervort, and J. M. Lourtioz, Phys. Rev. B **60**, 5851 (1999).
[14] J. Weber and M. I. Alonso, Phys. Rev. B **40**, 5683 (1989).
[15] G. Bremond, M. Serpentine, A. Souifi, G. Guillot, B. Jacquier, M. Abdallah, I. Berbezier, and B. Joyce, Microelectron. J. **30**, 357 (1999).
[16] O. G. Schmidt, C. Lange, and K. Eberl, Phys. Status Solidi B **215**, 319 (1999).
[17] E. R. Glaser, B. R. Bennett, B. V. Schanabrook, and R. Magno, Appl. Phys. Lett. **68**, 3614 (1996).
[18] R. Apetz, L. Vescan, A. Hartmann, C. Dieker, and H. Lueth, Appl. Phys. Lett. **66**, 445 (1995).
[19] Y. P. Varshni, Physica (Amsterdam) **34**, 149 (1967); J. I. Pankove, *Optical Processes in Semiconductors* (Prentice–Hall, Englewood, NJ, 1971), p. 25.
[20] Y. M. Mo, D. E. Savage, B. S. Swartzentruber, and M. G. Lagally, Phys. Rev. Lett. **65**, 1020 (1990).
[21] G. G. Qin, A. P. Li, B. R. Zhang, and B. C. Li, J. Appl. Phys. **78**, 2006 (1995).
[22] G. G. Qin, G. F. Bai, A. P. Li, S. Y. Ma, Y. K. Sun, B. R. Zhang, and Z. H. Zong, Thin Solid Films **338**, 131 (1999).
[23] O. G. Schmidt, C. Lange, and K. Eberl, Phys. Status Solidi B **215**, 319 (1999).
[24] A. A. Shklyaev and M. Ichikawa, Appl. Phys. Lett. **80**, 1432 (2002).
[25] K. S. Min, K. V. Shcheglov, C. M. Yang, H. A. Atwater, M. L. Brongersma, and A. Polman, Appl. Phys. Lett. **68**, 2511 (1996).
[26] W. M. Duncan, P. H. Chang, B. Y. Mao, and C. E. Chen, Appl. Phys. Lett. **51**, 773 (1987).
[27] T. Sekiguchi, V. V. Kveder, and K. Sumino, J. Appl. Phys. **76**, 7882 (1994).